JOURNAL OF NANO- AND ELECTRONIC PHYSICS
Vol. **17** No 1, 01021(6pp) (2025)

ЖУРНАЛ НАНО- ТА ЕЛЕКТРОННОЇ ФІЗИКИ
Том **17** № 1, 01021(6cc) (2025)

OPEN ACCESS

REGULAR ARTICLE

Characteristics of a Source of Synchronous Fluxes of UV Radiation and Zink Nanoparticles, Promising for Biomedical Engineering

O.K. Shuaibov,* ✉ iD, O.Y. Minya, R.V. Hrytsak, A.O. Malinina, O.M. Malinin

Uzhhorod National University, 88000 Uzhhorod, Ukraine

(Received 18 December 2024; revised manuscript received 18 February 2025; published online 27 February 2025)

The study investigates the properties of an overstressed nanosecond discharge between zinc electrodes in argon at pressures of p_{Ar} = 101.3 kPa. Under the influence of a strong electric field, microexplosions occurring at inhomogeneities on the electrode surfaces result in the release of zinc vapor into the discharge gap. This phenomenon creates favorable conditions for the formation of zinc-based nanostructures, which can subsequently be deposited onto a rigid dielectric substrate placed near the discharge gap. The spectral properties of the discharge were analyzed in the central area of the gap, where the electrode separation was kept at 2 mm. The excitation of primary plasma components, consisting of an argon-zinc vapor mixture, occurs at high values of the reduced electric field parameter (*E*/*N*), where (*E*) represents the electric field strength and (*N*) denotes particle concentration. These excited components, which are deposited outside the plasma region, play a role in the formation of zinc nanostructures on the surface. The study also explores the optimization of time-averaged ultraviolet (UV) radiation emitted from the point discharge source by adjusting the voltage of the high-voltage modulator and the pulse repetition rate. Numerical simulations of discharge plasma parameters in argon-zinc vapor mixtures at atmospheric pressure were conducted by solving the Boltzmann kinetic equation for the electron energy distribution function (EEDF). The simulations provided values for the mean electron energy, electron temperature, electron density, and rate constants as functions of the reduced electric field parameter (*E*/*N*), which were consistent with the experimental observations of the discharge.

Keywords: Nanosecond discharge, Argon, Zinc, Emission spectrum, Plasma, Numerical simulation, Plasma parameters.

DOI: 10.21272/jnep.17(1).01021

PACS numbers: 52.80. − s, 51.50. + v, 52.80.Tn, 52.90. + z, 52.80.Mg, 79.60.Jv

1. INTRODUCTION

When the distance between electrodes decreases from 5 mm to 0.5 mm, the plasma spectra generated by high-current nanosecond discharges at a pressure of 101 kPa are dominated by spectral lines corresponding to atoms and ions of electrode materials such as copper, iron, and zinc [1]. In the overvoltage regime of the interelectrode gap, "runaway electrons" are observed in the plasma, accelerating to energies corresponding to the amplitude of the voltage pulse [2, 3]. Under the influence of a "runaway electron" beam, which facilitates preionization, a uniform discharge with a non-uniform electric field forms in the discharge gaps, making it suitable for compact UV lamps with a plasma volume of less than 10 mm^3.The optical and energy characteristics of "point" UV lamps based on metal vapor from electrodes of unipolar and bipolar overstressed nanosecond discharges are presented in [4] and [5], respectively.Bipolar discharge reduces the impulse voltage by half relative to grounded components and ensures more uniform electrode material consumption, promoting ecton formation and the release of electrode material vapor into the plasma [6]. Island-like thin-film nanostructures made of copper and zinc oxides are synthesized from the vapor of electrode materials and air degradation products, and these structures can be deposited onto solid dielectric substrates [7, 8].

The study [9] found that continuous UV illumination of the substrate with a mercury lamp during the synthesis of nanopyramids from zinc oxide thin film nanostructures leads to a reduction in their resistance.

The analysis of emission characteristics of the bipolar overvoltage discharge in atmospheric air between zinc electrodes revealed that it serves as a selective source of radiation in the 200-230 nm range [10]. This radiation serves as a means for automatically illuminating zinc oxide nanostructure films with UV light during their synthesis. A high-voltage nanosecond discharge between copper or zinc electrodes produces plasma, which not only emits bactericidal UV radiation (200-280 nm) but also releases copper or zinc oxide nanoparticles with potent antibacterial properties [11]. The work [12] highlights the practical value of pure metal nanoparticles. Specifically, the study presents results on composite films with copper nanoparticles, synthesized via electrical explosion of conductors.

* Correspondence e-mail: alexsander.shuaibov@uzhnu.edu.ua

Cite this article as: O.K. Shuaibov et al., *J. Nano- Electron. Phys.* 17 No 1, 01021 (2025) https://doi.org/10.21272/jnep.17(1).01021

These films exhibit high efficiency against *Staphylococcus aureus* and show potential as radiation shielding materials.In [13], the potential of using transition metal oxide nanoparticles for biofuel production is emphasized. Catalysts based on these nanoparticles accelerate reactions, increasing biodiesel yields. Optimizing the synthesis of zinc-based thin film nanostructures requires enhancing the performance of the gas discharge reactor with argon as a buffer gas, enabling the deposition of island-like pure zinc films onto dielectric substrates under controlled UV illumination. The article discusses the investigation of electrical and optical properties of the overvoltage nanosecond discharge between zinc electrodes at argon pressure (p_{Ar} = 101.3 kPa). The results demonstrate the potential of using this process as a source of UV bactericidal radiation for the synthesis of zinc oxide nanostructures and the production of fine zinc powder.

2. METHODOLOGY AND TECHNIQUE OF THE EXPERIMENT

The characteristics of the overvoltage nanosecond discharge were studied using the experimental setup described in [1, 10]. The discharge cell schematic can be found in [1]. The nanosecond overvoltage discharge between zinc electrodes was initiated in a sealed acrylic chamber, with a distance between the electrodes of d = 2 mm.

Bipolar high-voltage pulses with a duration of 50-150 ns and an amplitude of ±(20-40) kV, applied at a repetition frequency of 150 Hz, were used to initiate the discharge in the electrodes of the discharge cell. The voltage oscillograms across the discharge gap and current pulse waveforms were recorded using a wideband capacitive voltage divider, a Rogowski coil, and a wideband oscilloscope (6ЛОР-04). By graphically multiplying the current and voltage pulse waveforms, the time-dependent distribution of pulsed energy contribution to the nanosecond discharge plasma was determined. Integration of the pulsed power over time provided an estimate of the electrical energy delivered to the discharge plasma during each cycle of voltage and current pulses.

The plasma emission, recorded in the spectral range λ = 196-663 nm, was directed through the entrance slit of a spectrometer with a diffraction grating of 1200 lines/mm. A photomultiplier ФЕП-106, connected to a DC amplifier, was used to register the emission at the spectrometer output. The signal from the amplifier was transmitted to an analog-to-digital converter and then to a computer for further processing.

The discharge chamber was first evacuated using a forevacuum pump to a residual pressure of 10 Pa. Afterward, argon was introduced into the chamber, reaching pressures of 13.3 or 101.3 kPa. The metallic cylindrical electrodes had a diameter of 5 mm, with a uniform radius of curvature of 3 mm at their working end. The volume of the discharge was influenced by the repetition frequency of the voltage pulses. The "spot discharge" mode occurred exclusively at pulse repetition frequencies within the range of f = 40-150 Hz.

The power of the discharge plasma emission was measured using a UV absolute radiation power meter ТКА-ПКМ, which allows measurements in the spectral range of 200-400 nm.

3. SPATIAL, ELECTRICAL AND SPECTRAL CHARACTERISTICS

The oscillograms for an overvoltage nanosecond discharge between Zn electrodes in argon (p_{Ar} = 13.3-101.3 kPa, d = 2 mm) closely resembled those observed for a similar discharge with copper electrodes [10]. Figure 1 displays representative oscillograms of current, voltage, pulsed power, and energy contribution to the plasma for a single discharge pulse occurring between zinc electrodes in argon.

The current and voltage oscillograms exhibited damped oscillations with a duration of approximately 7-10 ns, caused by an impedance mismatch between the high-voltage modulator's output resistance and the load resistance. The total duration of the voltage oscillations across the gap, along with the discharge current, extended up to 400 ns. Each individual voltage oscillation lasted 7-10 ns, while the current oscillations spanned about 70 ns. At the onset of the discharge, the voltage drop across the electrodes reached a peak of approximately + 4 kV, corresponding to a current of ± 30 A.

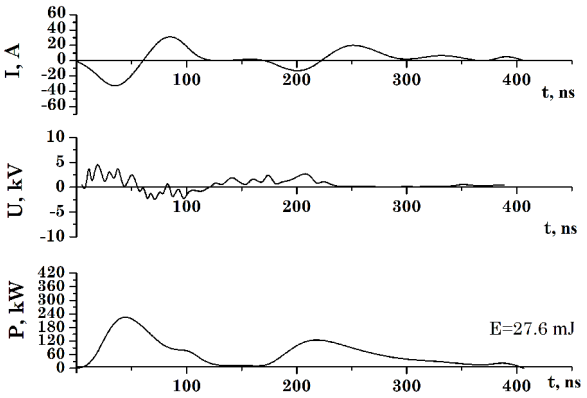

Fig. 1 – Oscillograms of current, voltage, pulsed power, and energy deposition into the plasma for a single pulse of an overvoltage nanosecond discharge at an electrode gap of d = 2 mm and argon pressure of p_{Ar} = 13.3 kPa

The discharge pulse power was determined by graphically multiplying the voltage and current oscillograms, as shown in Figure 1. By integrating the pulse power over the discharge duration, the energy contribution to the plasma from a single pulse was calculated. The peak discharge power reached 230 kW, delivering an energy input of up to 28 mJ per pulse to the plasma.

At atmospheric pressure (p = 101.3 kPa) with the same interelectrode distance (d = 2 mm), the shape of the voltage and current oscillograms remained largely unchanged, although the electrical parameters increased in magnitude. The maximum voltage drop across the electrodes rose to ± 7-8 kV, the current peaked at ± 100 A, and the pulsed power reached 1.2 MW, resulting in an energy contribution of approximately 167 mJ per pulse to the plasma.

Figure 2 presents the emission spectra of an overvoltage nanosecond discharge at various argon

pressures, while Table 1 summarizes the identification of spectral lines (bands) and their relative intensities. References [14, 15] were used to interpret the spectral data.

The primary features in the UV spectrum of plasma radiation were the spectral lines of neutral zinc atoms and singly ionized zinc ions. These lines were observed within the ranges of 206-280 nm and 330-335 nm (Zn I lines). The most intense lines of ionic zinc included 206.20 and 209.99 nm (Zn II), while the strongest atomic zinc lines were 213.85, 330.25, and 334.50 nm (Zn I), aligning closely with the spectral characteristics of a zinc vapor lamp as detailed in [16].

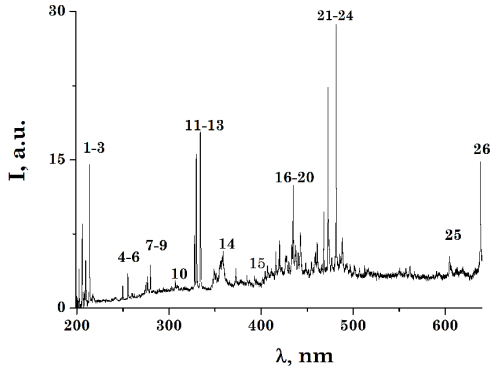

Fig. 2 – Emission spectrum of an overvoltage nanosecond discharge between zinc electrodes at an argon pressure of p_{Ar} = 101.3 kPa

In the radiation spectra of plasma generated by a bipolar overvoltage nanosecond discharge in air, or in a mixture of air with a small fraction of water vapor at a total pressure of 103.3 kPa (d = 1 mm), two distinct groups of intense lines dominated the UV range of 20-280 nm. The first group featured prominent ion lines, including 202.6 and 206.2 nm (Zn II), while the second group was characterized by strong atomic lines at 250.2 and 255.8 nm (Zn I) [1]. These findings differ from those obtained for a discharge in argon at a pressure of 13.3 kPa, likely due to variations in the buffer gas type, pressure, and ecton formation conditions.

A comparison of the effective cross-sections of the zinc atomic spectral lines at 275.64 and 258.24 nm, as provided in [17], with experimental data revealed that the ratio of direct electronic excitation cross-sections at an electron energy of 30 eV was 0.5, while the experimentally measured intensity ratio was 1.1. Similarly, for the lines at 328.23 and 307.20 nm, the calculated cross-section ratio was 1.0, which correlated closely with the experimental intensity ratio. These significant discrepancies suggest that direct electron impact is not the primary mechanism for populating the upper energy levels of these zinc atomic lines in this experimental setup.

As the argon pressure increased to atmospheric levels, improved impedance matching between the high-voltage modulator and the discharge enhanced energy transfer to the plasma. This resulted in a higher energy contribution and increased emission intensity of the spectral lines. However, the relative intensity distribution and other spectral patterns remained similar to those observed at an argon pressure of 13.3 kPa.

Table 1 – Identification results for the radiation spectrum of nanosecond discharge plasma; Zn electrodes, electrode distance 2 mm; argon pressure 1 atm (101.32 kPa); U_{Fep} = 1060 V

No	λ_{tab}, nm	I_{exp}, a.u.	Object	$E_{low.}$, eV	$E_{up.}$, eV	Lower term	Upper term
1	206.20	8.74	Zn II	0	6.01	$3d^{10}4s\ ^2S_{1/2}$	$3d^{10}4p\ ^2P^0_{1/2}$
2	209.99	4.85	Zn II	6.11	12.02	$3d^{10}4p\ ^2P^0_{3/2}$	$3d^{10}4d\ ^2D_{5/2}$
3	213.85	13.08	Zn I	0	5.79	$3d^{10}4s^2\ ^1S_0$	$3d^{10}4s4p\ ^2P^0_1$
4	250.19	2.35	Zn I	6.01	10.96	$3d^{10}4p\ ^2P^0_{1/2}$	$3d^{10}5s\ ^2S_{1/2}$
5	255.79	3.97	Zn II	6.11	10.96	$3d^{10}4p\ ^2P^0_{3/2}$	$3d^{10}5s\ ^2S_{1/2}$
6	258.24	1.12	Zn I	4.02	8.82	$3d^{10}4s4p\ ^3P^0_1$	$3d^{10}4s6d\ ^3D_2$
7	275.64	2.65	Zn I	4.00	8.50	$3d^{10}4s\ 4p\ ^3P^\circ_0$	$3d^{10}4s\ 5d\ ^3D_1$
8	277.08	3.16	Zn I	4.02	8.50	$3d^{10}4s\ 4p\ ^3P^\circ_1$	$3d^{10}4s\ 5d\ ^3D_2$
9	280.08	4.11	Zn I	4.07	8.50	$3d^{10}4s\ 4p\ ^3P^\circ_2$	$3d^{1}04s\ 5d\ ^3D_3$
10	307.206	2.49	Zn I	4.07	8.11	$3d^{10}4s4p\ ^3P^0_2$	$3d^{10}4s6s\ ^3S_1$
11	328.23	7.43	Zn I	4.00	7.78	$3d^{10}4s4p\ ^3P^0_0$	$3d^{10}4s4d\ ^3D_1$
12	330.25	15.57	Zn I	4.02	7.78	$3d^{10}4s4p\ \ ^3P^\circ_1$	$3d^{10}4s4d\ ^3D_2$
13	334.50	17.89	Zn I	4.07	7.78	$3d^{10}4s4p\ ^3P^\circ_2$	$3d^{10}4s4d\ ^3D_3$
14	357.69	5.08	N_2	Second positive system $C^3\Pi_u^+$-$B^3\Pi_g^+$ (0;1)			
15	395.27	2.75	Ar II	19.97	24.28	$4p'\ ^2F^0_{7/2}$	$5s'\ ^2D_{5/2}$
16	404.56	3.73	Ar II	18.29	21.35	$3d\ ^4P_{3/2}$	$4p'\ ^2P^0_{3/2}$
17	415.85	5.68	Ar I	11.55	24.53	$4s\ \ [1\ 1/2]^0_2$	$5p\ [1\ 1/2]_2$
18	420.19	7.01	Ar II	16.81	19.76	$4s\ ^4P_{1/2}$	$4p\ ^2D^0_{3/2}$
19	430.01	4.73	Ar I	11.62	14.51	$4s\ \ [1\ 1/2]^0_1$	$5p\ [2\ 1/2]_2$
20	443.38	7.03	Ar II	21.37	24.16	$3d'\ ^2D_{5/2}$	$(^3P_2)\ 4f[3]^0_{7/2}$
21	468.22	9.76	Ar II	18.49	21.13	$3d\ ^2F_{7/2}$	$4p'\ ^2F^0_{7/2}$
22	472.21	22.97	Zn I	4.02	6.65	$3d^{10}4s4p\ ^3P^\circ_1$	$3d^{10}4s5s\ ^3S_1$
23	481.05	28.72	Zn I	4.07	6.65	$3d^{10}4s4p\ ^3P^\circ_2$	$3d^{10}4s5s\ ^3S_1$
24	492.40	4.5	Zn II	12.02	14.53	$3d^{10}4d\ ^2D_{5/2}$	$3d^{10}4f\ ^2F^0_{7/2}$
25	603.21	5.04	Ar I	13.08	15.13	$4p\ \ [2\ 1/2]_3$	$5d\ \ [3\ 1/2]^0_4$
26	638.47	14.84	Ar I	12.91	14.85	$4p\ \ [1/2]_1$	$6s\ \ [1\ 1/2]_1$

The majority of the energy in an overvoltage nanosecond discharge is initially transferred to the plasma's electron component, which subsequently distributes the energy to atoms in excited states and to ions. Therefore, the mechanisms responsible for generating excited zinc atoms and ions likely involve processes such as excitation and ionization by electron impact from metastable or ground states of the corresponding ions, as well as dielectronic recombination [18]. The effective cross-sections for electron-impact excitation of transition metal ions, including zinc ions, are substantial, reaching values of approximately 10^{-16} cm² [19].

Figure 3 illustrates the dependence of UV radiation intensity from an overvoltage nanosecond discharge between zinc electrodes in medium-pressure argon on the charging voltage of the high-voltage modulator's working capacitor. As the charging voltage increased from 13 kV to 20 kV, the most significant rise in UV radiation intensity was observed in the 315-400 nm spectral range, where the maximum power density reached approximately 2.1 mW/m². In the bactericidal spectral range (200-280 nm), the maximum power density of UV radiation remained below 1 mW/m². However, increasing the pulse repetition rate beyond 100-150 Hz caused considerable heating of the discharge device, limiting its operation to short durations.

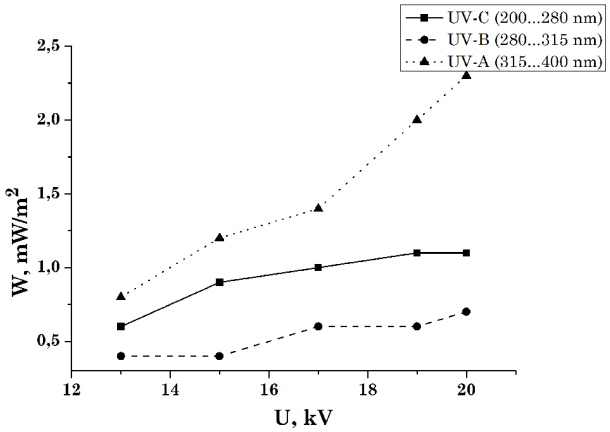

Fig. 3 – Variation in average UV radiation intensity across the UV-C, UV-B, and UV-A ranges as a function of the charging voltage of the high-voltage modulator's capacitor in an overvoltage nanosecond discharge at $f = 80$ Hz, $p_{Ar} = 7$ kPa, $d = 2$ mm

Raising the pulse repetition frequency from 350 Hz to 1000 Hz led to a notable increase in UV radiation intensity across all spectral ranges. The most significant enhancement was in the 315-400 nm range, where the intensity increased from 0.5 mW/m² to 4.5 mW/m². In the bactericidal spectral range, the UV radiation intensity rose from 1.0 mW/m² at 350 Hz to 1.5 mW/m² at 1000 Hz.

4. PLASMA PARAMETERS

The plasma parameters were determined using the Bolsig+ software [20]. The model incorporated the following electron collision processes with zinc and argon atoms: elastic scattering, excitation of zinc atom energy levels (with threshold energies of 4.02, 5.79, 17.61, and 23.55 eV), zinc atom ionization (threshold energy of 9.40 eV), excitation of argon atom energy levels (threshold energy of 11.50 eV), argon atom ionization (threshold energy of 15.80 eV), as well as electron-electron and electron-ion collisions. Excitation of the zinc atom energy levels contributed to the emission of spectral lines in the 236-604 nm range.

The effective cross sections for exciting the metastable levels 4^3P_0 and 4^3P_2 of the zinc atom were maximal in the range of $(0.3\text{-}1.4) \times 10^{-16}$ cm² at an incident electron energy of 4.5 eV. The excitation functions showed a characteristic behavior: a sharp increase from the threshold to the peak followed by a gradual decline beyond the maximum.

The range of the reduced electric field strength parameter $E/N = 1 - 2500$ Td ($1 \times 10^{-17} - 2.5 \times 10^{-15}$ cm²) included values relevant to the overvoltage nanosecond discharge in an argon-zinc vapor mixture with a component ratio of 101300:100 Pa. At a total pressure of $p = 101400$, the corresponding E/N values were 2459 and 1229 Td at 80 ns and 100 ns after discharge ignition, respectively. During this period, the voltage and current pulse amplitudes reached 60 kV and 150 A, and 30 kV and 130 A, respectively.

Figure 4 illustrates the dependence of the average electron energy in a plasma of an argon-zinc vapor mixture (Ar:Zn = 101300:100 Pa) at $p = 101400$ Pa, as a function of the reduced electric field strength.

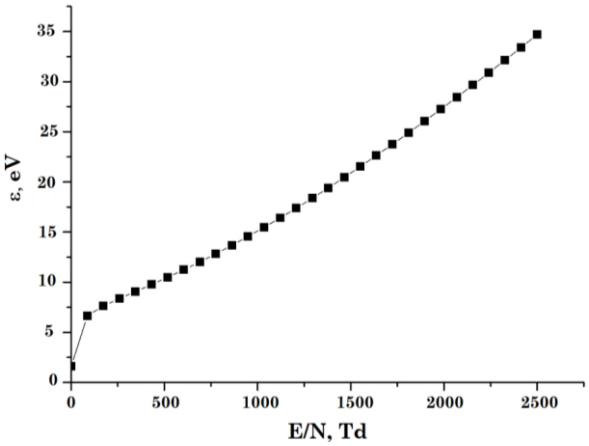

Fig. 4 – Dependence of the average electron energy in a discharge on a Zn-Ar mixture (100-101000 Pa) on the reduced electric field strength at a total pressure of $p = 101400$ Pa

The average energy of electrons in the gas-vapor mixture (Ar:Zn = 101300:100 Pa) increased from 1.625 eV to 34.69 eV as the reduced electric field strength (E/N) rose from 1 to 2500 Td (Fig. 4). A rapid increase in the rate of energy growth was observed within the range of $E/N = 1\text{-}50$Td. At 80 ns and 100 ns after the discharge initiation, the average electron energy was 34.69 eV and 17.38 eV, respectively, corresponding to plasma temperatures of 402.404 Td and 201.608 Td.

The electron drift velocity reached 1.2×10^6 m/s at 80 ns and 7×10^5 m/s at 100 ns under a discharge electric field strength of 6×10^7 V/m. The electron

concentration was 3.98×10^{19} m^{-3} at 80 ns and 3.45×10^{20} m^{-3} at 100 ns. These values correspond to current densities of 7.65×10^{6} A/m^2 and 6.63×10^{6} A/m^2, respectively, on electrode surfaces with an area $S = 0.196 \times 10^{-6}$ m^2.

At 80 ns, the reduced electric field strength in the discharge gap was $E/N = 2459$ Td, while at 100 ns, it was $E/N = 1229$ Td. These conditions significantly influenced the discharge parameters and electron dynamics.

The rate constants for electronic processes varied between $k = 10^{-12}$ and 10^{-23} m^3/s, which are linked to the absolute effective cross sections for the corresponding processes (Fig. 5). For zinc atoms, the rate constants ranged from 0.6379×10^{-17} to 0.1055×10^{-17} m^3/s at a reduced electric field strength of $E/N = 2500$ Td in the discharge gap at 80 ns, and from 0.3808×10^{-17} to 0.1002×10^{-12} m^3/s at $E/N = 1229$ Td in the discharge gap at 100 ns.The rate constants for the excitation of the energy level of the zinc atom ($E_{thr} = 5.02$ eV) were 0.7428×10^{-14} m^3/s at $E/N = 2500$ Td and 0.5072×10^{-12} m^3/s at $E/N = 1229$ Td.

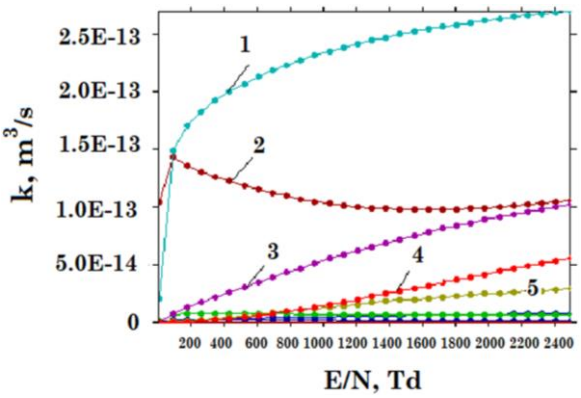

Fig. 5 – Dependencies between the rate constants for electron collisions with zinc and argon atoms and the E/N parameter in a Zn:Ar mixture discharge (100:101300 Pa) at a total pressure of 101400 Pa: 1 – elastic scattering with argon atoms, 2 – elastic scattering with zinc atoms, 3 – ionization of zinc atoms (threshold energy 9.4 eV), 4 – ionization of argon atoms (threshold energy 15.80 eV), 5 – excitation of argon atom energy levels (threshold energy 11.50 eV)

The discharge power losses in a zinc vapor-argon mixture, due to inelastic electron collisions with the components, were maximized at a reduced electric field strength of 2500 Td. These losses were predominantly attributed to the ionization of argon atoms (threshold energy 15.8 eV) and the excitation of their energy levels (threshold energy $E_{thr} = 11.50$ eV), accounting for 27.92 % and 10.54 %, respectively. When the reduced electric field strength decreased to $E/N = 1229$ Td, 100 ns after the discharge gap breakdown, the losses increased to 37.35 % and 21.31 %. The maximum discharge power loss, 76.31 %, occurred during the excitation of argon atom energy levels at a reduced electric field strength of 87.2 Td, while the zinc atom's loss was 48.6 % (threshold energy of 4.00 eV) at 1 Td.

5. CONCLUSIONS

Thus, it has been determined that in argon pressures ranging from 13.3 to 101.3 kPa, a spatially uniform overvoltage nanosecond discharge was initiated between zinc electrodes with a 2 mm interelectrode gap. The discharge exhibited a pulsed electrical power of at least 230 kW and an energy contribution to the plasma of at least 28 mJ (at $p_{Ar} = 13.3$ kPa). At atmospheric argon pressure, these values increased to 1200 kW and approximately 167 mJ, respectively.

Analysis of the spectral properties of plasma in an "argon-zinc" gas-vapor mixture revealed that the most intense spectral lines corresponded to zinc atoms and singly charged zinc ions. The primary mechanisms for the formation of excited atoms and ions in this discharge appear to be stepwise excitation processes of zinc atoms and ions by electrons, along with dielectronic recombination.

The consistent emission of intense UV radiation from zinc atoms and ions in the overvoltage plasma of a nanosecond discharge holds potential for influencing the electrical properties of nanostructured zinc films through irradiation of substrates and film nuclei.

The highest average electron energy in the "Argon-Zinc = 101300:100 Pa" gas-vapor mixture reached 34.69 eV, corresponding to a plasma temperature of 402.404 K. The highest electron concentration was 3.98×10^{9} m^{-3}, and the rate constants of the electron processes in the discharge varied between $k = 10^{-12}$ to 10^{-25} m^3/s, which is linked to the values of the absolute effective cross sections for the respective processes.

REFERENCES

1. O.K. Shuaibov, A.O. Malinina, O.M. Malinin, *New gas-discharge method for obtaining selective ultraviolet and visible radiation to the synthesis of nanostructures of transition metal oxides* (Uzhgorod: Publisher UzhNU "Goverla": 2019).
2. *Runaway electrons preionized diffuse discharge* (Ed. by V.F. Tarasenko) (New York: Nova Science Publishers Inc.: 2014).
3. G.A. Mesyac, M.I. Yalandin, *Phys.-Usp.* **189** No 7, 747 (2014).
4. E.Kh. Bakst, V.F. Tarasenko, Yu.V. Shut'ko, M.V. Erofeev, *Quantum Electron.* **42** No 2,153 (2012).
5. A.K. Shuaibov, A.Y. Minya, Z.T. Gomoki, A.A. Malinina, A.N Malinin, *Surf. Eng. Appl. Electrochem.* **56** No 4, 510 (2020).
6. G.A. Mesyats, *Phys.-Usp.* **38** No 6, 567 (1995).
7. A. Voloshko, T.E. Itina, *Appl. Phys. B* **113**, 473 (2013).
8. A.K. Shuaibov, A.Y. Minya, A.A. Malinina., A.N. Malinin, V.V. Danilo, M.Yu. Sichka, I.V. Shevera, *Am. J. Mechan. Mater. Eng.* **2** No 1, 8 (2018).
9. A.Kh. Abduev, A.Sh. Asvarov, A.K. Akhmetov, R.M. Emyrov, V.V. Beliaev, *Tech. Phys. Lett.* **43** No 22, 40 (2017).
10. O.K. Shuaibov, A.I. Minya, M.P. Chuchman, A.O. Malinina, V.V. Danilo, Z.T. Homoki, *Ukr. J. Phys.* **63** No 9, 790 (2018).
11. Palani Geetha, Kannan Karthik, D. Radhika, P. Vijayakumar, K. Pakiyaraj, *Phys. Chem. Solid State* **21** No 4, 571 (2020).
12. V.V. Krivtsov, V.V. Kukla, V.V. Krivtsov, A.J. Shidlovskiy,

M.A. Bordyuk, *J. Nano- Electron. Phys.* **12** No 4, 04032 (2020).
13. P.P. Gohain, S. Paul, *J. Nano- Electron. Phys.* **14** No 3, 03005 (2022).
14. A.R. Striganov, N.S. Sventitsky, *Tables of spectral lines of neutral and ionized atoms* (M: Atomizdat: 1966).
15. *NIST Atomic Spectra Database Lines Form*.
16. S.I. Maximov, A.V. Kretinina, N.S. Fomina, L.N. Gall, *Sci. Instrum.* **25** No1, 36 (2015).
17. Yu.M. Smirnov, *Opt. Spectroscopy* **104** No 2, 159 (2008).
18. R. Shuker, Y. Binur, A. Szoke, *Phys. Rev. A* **12**, 212 (1975).
19. A.N. Gomonai, *J. Appl. Spectroscopy* **82** No 1, 17 (2015).
20. *BOLSIG+, Electron Boltzmann equation solver*.

Характеристики джерела синхронних потоків УФ-випромінювання та наночастинок цинку, перспективного для біомедичної інженерії

О.К. Шуаібов, О.Й. Миня, Р.В. Грицак, А.О. Малініна, О.М. Малінін

ДВНЗ «Ужгородський національний університет», 88000 Ужгород, Україна

Дослідження вивчає властивості перенапруженого наносекундного розряду між цинковими електродами в аргоні при тиску p_{Ar} = 101,3 кПа. Під впливом сильного електричного поля мікровибухи, що виникають на неоднорідностях поверхонь електродів, спричиняють виділення парів цинку в розрядний проміжок. Це явище створює сприятливі умови для формування наноструктур на основі цинку, які згодом можуть бути осаджені на жорстку діелектричну підкладку, розташовану поблизу розрядного проміжку. Спектральні властивості розряду аналізували в центральній зоні проміжку, де відстань між електродами становила 2 мм. Збудження основних компонентів плазми, що складається зі суміші аргону та парів цинку, відбувається за високих значень зниженого параметра електричного поля (*E*/*N*), де (*E*) – це напруженість електричного поля, а (*N*) – концентрація частинок. Ці збуджені компоненти, які осаджуються за межами області плазми, відіграють важливу роль у формуванні наноструктур цинку на поверхні. У дослідженні також розглядається оптимізація середнього за часом ультрафіолетового (УФ) випромінювання, що випускається точковим джерелом розряду, шляхом регулювання напруги високовольтного модулятора та частоти повторення імпульсів. Числове моделювання параметрів розрядної плазми в сумішах аргону та парів цинку при атмосферному тиску проводилося шляхом розв'язання кінетичного рівняння Больцмана для функції розподілу енергії електронів (EEDF). Моделювання дало значення середньої енергії електронів, температури електронів, густини електронів і констант швидкості як функцій зниженого параметра електричного поля (*E*/*N*), які узгоджувалися з експериментальним дослідженням розряду.

Ключові слова: Наносекундний розряд, Аргон, Цинк, Спектр випромінювання, Плазма, Числове моделювання, Параметри плазми.